

Computers and Electronics in Agriculture

Counting wheat heads using a simulation model

--Manuscript Draft--

Manuscript Number:	COMPAG-D-24-00458R2
Article Type:	Research Paper
Keywords:	Wheat head counting; simulation; Deep Learning; object detection
Corresponding Author:	Lingrang Kong, Ph.D. Shandong Agricultural University Taian, Shandong CHINA
First Author:	Xiaoyong Sun, Ph.D.
Order of Authors:	Xiaoyong Sun, Ph.D. Tianyou Jiang Jiming Hu Song Zuojie Yuheng Ge Yongzhen Wang Liu Xu Bing Jianhao Li Jinshan Zhou Ziyu Zhongzhen Tang Yan Zhao Jinyu Hao Changzhen Zuo Xia Geng Lingrang Kong, Ph.D.
Abstract:	Numerous studies have reported a significant positive correlation between wheat yield and the quantity of wheat heads. However, collecting data on wheat heads in the field poses a challenge for several reasons, including the uncontrollable nature of the environment, inconsistent data quality, and ambiguous data truth. To address these challenges, we developed a simulation strategy to replicate the conditions of a real wheat field, which enabled the data collection process to be conducted indoors over a short period. After applying grayscale image processing to process the simulated wheat images, we trained and tested nine deep learning models: Faster-RCNN, YOLOv7, YOLOv8, CenterNet, SSD, RetinaNet, EfficientDet, Deformable-DETR and DINO. Our results indicated that YOLOv7 performed the best ($R^2=0.963$, $RMSE=2.463$). We then compared our model trained on simulated wheat data to a model trained on real wheat data ($R^2=0.963$ vs 0.972 , $RMSE=2.463$ vs 2.692). We also achieved good model performance on five test sets: GWHD, SDAU2021-SDAU2024. The results demonstrated the efficacy of our simulation, which provides an efficient and convenient strategy for the precision agriculture community.
Suggested Reviewers:	Chrisbin James chris.james@uq.edu.au Shizhong Yang yszxlj@126.com Dongyan Zhang zhangdy@ahu.edu.cn

	Jatinder S. Sangha jatinder.sangha2@agr.gc.ca
	HaiYan Cen hycen@zju.edu.cn
Response to Reviewers:	



September 12, 2024

Dear Editor:

Enclosed is our manuscript entitled "**Counting wheat heads using a simulation model**" that we would like to be considered for publication in the *Computers and Electronics in Agriculture*.

Numerous studies have reported a significant positive correlation between wheat yield and the quantity of wheat heads. However, collecting data on wheat heads in the field poses a challenge for several reasons, including the uncontrollable nature of the environment, inconsistent data quality, and ambiguous data truth. To address these challenges, we collected real data from 2021 to 2023, and **developed a simulation strategy to replicate the conditions of a real wheat field, which enabled the data collection process to be conducted indoors over a short period**. Our results indicated that YOLOv7 performed the best ($R^2=0.963$, RMSE=3.949). We then compared our model trained on simulated wheat data to a model trained on real wheat data. The experimental results illustrated the efficacy of our simulation method, which was shown to provide an efficient and convenient strategy for the precision agriculture community.

All correspondence regarding this manuscript should be addressed to Dr. Lingrang Kong, National Key Laboratory of Wheat Improvement, College of Agronomy, Shandong Agricultural University, Tai'an, Shandong 271018, PR China. I can also be reached by telephone (+86 5388249278), or by Email (lkong@sdau.edu.cn).

Thank you for your consideration of our manuscript and we look forward to hearing from you.

Sincerely,

Lingrang Kong
Professor
National Key Laboratory of Wheat Improvement
College of Agronomy
Shandong Agricultural University
Taian, Shandong, P.R.China

Email: lkong@sdau.edu.cn

Response to the comments by the reviewers for the article:

Counting wheat heads using a simulation model

Xiaoyong Sun^{1,†}, Tianyou Jiang^{1,†}, Jiming Hu^{1,†}, Zuojie Song¹, Yuheng Ge¹, Yongzhen Wang¹, Xu Liu¹, Jianhao Bing¹, Jinshan Li¹, Ziyu Zhou¹, Zhongzhen Tang¹, Yan Zhao², Jinyu Hao¹, Changzhen Zuo¹, Xia Geng¹, Lingrang Kong^{2,*}

Dear Editor:

We would like to thank you and the reviewers for their precious comments and suggestions, so that we have been able to make a substantial improvement on the article.

Thank you!

Lingrang Kong
National Key Laboratory of Wheat Improvement
College of Agronomy
Shandong Agricultural University
Taian, Shandong, P.R.China

Answers to Reviewers' Comments and Questions:

Reviewer 1:

Question 1: *Should R2 be changed to R² in some charts? For example, Table 2, Figure 2 and etc.*

Reply: Thanks for the suggestion. We have modified R2 to R² in the manuscript, including Table 2 and Figure 2.

Highlights

1. A simulation model that replicates the real conditions of a wheat field was proposed.
2. Four wheat head data sets (GWHD2021, SDAU2021, SDAU2022, SDAU2023) were collected as the test data.
3. Nine deep learning models, including Faster-RCNN, YOLOv7, YOLOv8, CenterNet, SSD, RetinaNet, EfficientDet, Deformable-DETR and DINO, were trained and tested.
4. The results demonstrated the efficacy of our simulation.

1 **Counting wheat heads using a simulation model**

2

3 **Authors**4 Xiaoyong Sun^{1,†}, Tianyou Jiang^{1,†}, Jiming Hu^{1,†}, Zuojie Song¹, Yuheng Ge¹, Yongzhen Wang¹, Xu
5 Liu¹, Jianhao Bing¹, Jinshan Li¹, Ziyu Zhou¹, Zhongzhen Tang¹, Yan Zhao², Jinyu Hao¹, Changzhen
6 Zuo¹, Xia Geng¹, Lingrang Kong^{2,*}

7

8 ¹Agricultural Big-Data Research Center, College of Information Science and Engineering,
9 Shandong Agricultural University, Tai' an, Shandong 271018, PR China.10 ²National Key Laboratory of Wheat Improvement, College of Agronomy, Shandong Agricultural
11 University, Tai' an, Shandong 271018, PR China.

12

13 [†]These authors contributed equally to this article.

14

15 **Corresponding Author:** Lingrang Kong (lkong@sdau.edu.cn)16 National Key Laboratory of Wheat Improvement, College of Agronomy, Shandong Agricultural
17 University, Tai' an, Shandong 271018, PR China.

18

19 **Keywords:** wheat head counting; simulation; deep learning; object detection

20 **Abstract**

21 Numerous studies have reported a significant positive correlation between wheat yield and the
22 quantity of wheat heads. However, collecting data on wheat heads in the field poses a challenge for
23 several reasons, including the uncontrollable nature of the environment, inconsistent data quality,
24 and ambiguous data truth. To address these challenges, we developed a simulation strategy to
25 replicate the conditions of a real wheat field, which enabled the data collection process to be
26 conducted indoors over a short period. After applying grayscale image processing to process the
27 simulated wheat images, we trained and tested nine deep learning models: Faster-RCNN, YOLOv7,
28 YOLOv8, CenterNet, SSD, RetinaNet, EfficientDet, Deformable-DETR and DINO. Our results
29 indicated that YOLOv7 performed the best ($R^2=0.963$, RMSE=2.463). We then compared our
30 model trained on simulated wheat data to a model trained on real wheat data ($R^2=0.963$ vs 0.972,
31 RMSE=2.463 vs 2.692). We also achieved good model performance on five test sets: GWHD,
32 SDAU2021-SDAU2024. The results demonstrated the efficacy of our simulation, which provides
33 an efficient and convenient strategy for the precision agriculture community.

34

35

36

37 **Introduction**

38 Wheat, which originated from Northern Africa or Western Asia, is one of the earliest cultivated
39 crops in human history (Balfourier et al., 2019; Lev-Miram et al., 2023). Due to its remarkable
40 adaptability, it is extensively cultivated across a diverse range of regions worldwide. Reports
41 suggest that as a fundamental dietary staple, wheat is eaten by approximately 35–40% of the global
42 population (Gupta et al., 2023). The impact of extreme climatic conditions on food security has
43 given rise to a pressing need to enhance wheat yields (Myers et al., 2017; Dhankher et al., 2018;
44 Tesfaye et al., 2021).

45

46 Numerous studies have found a significant positive correlation between wheat yield and the
47 quantity of wheat heads (Liu et al., 2022; Zhao et al., 2022; Rezaei et al., 2023), which implies that
48 the number of wheat heads per unit area plays a pivotal role when estimating wheat yield. Due to
49 the complexities encountered in real wheat fields, the swift and accurate detection and counting of
50 wheat heads remain persistent challenges (David et al., 2020; David et al., 2023). Conventional
51 manual counting methods are not only time-consuming, but are also prone to human error (Liu
52 et al., 2016). It has therefore become paramount to explore efficient methods for counting wheat
53 heads to improve yield estimations (Wu et al., 2023).

54

55 Following the rapid developments in computer vision technology, image processing and feature
56 extraction have started to become key technologies for wheat head detection (Zhu et al., 2016;
57 Hartley et al., 2021). In 2018, Fernandez Gallego et al. (Fernandez-Gallego et al., 2018) proposed
58 an automatic wheat head counting algorithm to estimate the head density under field conditions,
59 based on zenithal color digital images taken from above the crop under natural lighting conditions.
60 The results demonstrated a high success rate (> 90%) between the algorithm counts and the manual
61 (image-based) head counts. Later, an automatic thermal head counting system (Fernandez-Gallego
62 et al., 2019) was proposed, as well as a system that used RGB (red, green, blue) images (Fernandez-

63 Gallego et al., 2020) to count the number of wheat heads, which achieved R^2 values of 0.80 and
64 0.89, respectively. Zhou et al. (Zhou et al., 2018) counted wheat heads under field conditions using
65 multi-feature optimization and the twin-support-vector-machine segmentation (TWSVM-Seg)
66 model, reporting a precision of 0.79–0.82.

67

68 In recent years, deep learning has played an important role in the development of smart agriculture
69 (Darwin et al., 2021), and object detection models have been adopted to recognize and count wheat
70 heads (Dandrifosse et al., 2022), a task that is of practical importance in terms of predicting wheat
71 yields (Romanovska et al., 2023), planning the planting process (Huang et al., 2022), and obtaining
72 excellent varieties of wheat (Sun et al., 2023). Convolutional neural networks (CNNs) are leading
73 the way in the area of image-based phenotyping (Li et al., 2022). Madec et al. (Madec et al., 2019)
74 explored the potential of CNNs in accurately determining head density using high-resolution RGB
75 images captured from a nadir perspective. Their results demonstrated that Faster-RCNN and *in situ*
76 counting gave similarly high values for heritability ($H^2 \approx 85\%$). Xu et al. (Xu et al., 2020) counted
77 wheat heads using K-means clustering segmentation and a CNN, achieving an R^2 value of 0.96 and
78 reducing the workload associated with manual annotation.

79

80 However, collecting data on wheat heads poses a challenge in the field (Sadeghi-Tehran
81 et al., 2019), and there are many factors that can affect the quality of the data. Firstly, the data
82 collection environment is uncontrollable (Long et al., 2015). Many factors, including the weather,
83 illumination, and seasonal changes, have a direct impact on the collection process. Since the mature
84 stage of a wheat head lasts only around 10 days, it is difficult to collect thousands of images, or
85 even tens of thousands, in a very short time (Liu et al., 2022). Secondly, the quality of the data is
86 uncontrollable in the field. The different phenomics of wheat (such as the height, color, and shape)
87 and related camera configurations can result in low-quality images, with blurring, occlusion, and
88 uneven lighting (Yue et al., 2018). In addition, data labeled as ground truth are not in fact accurate;

89 it is very hard to correctly annotate crowded wheat heads in an image that includes overlapping and
90 incomplete sections (Wang et al., 2021), meaning that it is impossible to obtain a real count of
91 wheat heads for the first step in training the model.

92

93 To address these challenges, we propose a simulation strategy that replicates the real conditions of
94 a wheat field. This enables the data collection process to be conducted entirely indoors. After
95 applying grayscale image processing to the simulated wheat images, we trained and tested nine
96 deep learning models: Faster-RCNN (Ren et al., 2015), YOLOv7 (Wang et al., 2023), YOLOv8,
97 CenterNet (Duan et al., 2019), SSD (Liu et al., 2016), RetinaNet (Lin et al., 2017), EfficientDet
98 (Tan et al., 2020), Deformable-DETR (Zhu et al., 2010) and DINO (Zhang et al., 2022). Our results
99 indicated that YOLOv7 performed the best ($R^2=0.963$, RMSE=2.463). We then compared our
100 model trained on simulated wheat data to a model trained on real wheat data. We also achieved
101 good model performance on five test sets: GWHD, SDAU2021-SDAU2024. The experimental
102 results illustrated the efficacy of our simulation method, which was shown to provide an efficient
103 and convenient strategy for the precision agriculture community.

104

105 **Materials and Methods**

106 **1. Data collection**

107 All the simulated wheat data were collected using a hand-held camera (EOS 70D, Canon, Japan).
108 The real wheat data were derived from the Global Wheat Head Detection 2021 dataset
109 (GWHD2021), collected over a four-year period from 2021 to 2024 (SDAU2021, SDAU2022,
110 SDAU2023, SDAU2024). The SDAU 2021 dataset were collected using an unmanned aerial
111 vehicle (DJI Genie 4 PRO V2.0, DJI, China), flown at a consistent speed of approximately 1 m/s
112 at a flight height of between 1.6 and 1.8 m. The PT head camera angle was set to a vertical
113 downward position, with a 55° tilt. We controlled the drone manually during data collection, using
114 DJI GO 4 as the flight control software. The SDAU2022-2024 datasets were collected from the

115 ground using a handheld camera, with a height similar to the flight height of the unmanned aerial
116 vehicle. These real wheat data were collected from the Science and Technology Innovation Park of
117 Shandong Agricultural University (SDAU). The SDAU2021 dataset consists of images of green
118 wheat, while the SDAU2022 and SDAU2024 datasets contain images of yellow wheat. In the
119 SDAU2023 dataset, the images reflected the developmental phases of wheat, portraying its
120 transition from the green stage to the yellow stage. Annotation of the collected data was performed
121 using LabelImg ([LabelImg program](#)). It was observed that the initial data annotation in the
122 GWHD2021 dataset lacked the desired accuracy, and a meticulous re-labeling process was
123 therefore conducted on the 100 images used in the experiment to fully improve the precision of
124 annotation. Finally, all images underwent grayscale processing before being fed into the deep
125 learning models.

126

127 **2. Training, validation, and test data**

128 The training dataset consists of a total of 800 images, all of which were collected using the proposed
129 simulation process for wheat images, which was carried out indoors. 200 images of simulated wheat
130 were used as the validation dataset. The test dataset consists of five parts: (i) 100 images randomly
131 selected from the GWHD2021 dataset; (ii) 100 images of green wheat from the SDAU2021 dataset;
132 (iii) 30 images of yellow wheat from the SDAU2022 dataset; (iv) 100 images of wheat, turning
133 from green to yellow, from the SDAU2023 dataset. (v) 1000 images of yellow wheat from
134 SDAU2024 dataset. Specifically, wheat images selected from the GWHD dataset were in different
135 colors, relatively high resolution and can be recognized by human eye.

136

137 **3. Model comparison**

138 In our quest to identify the most suitable model for wheat head counting, we conducted extensive
139 training and testing, and considered nine different deep learning models: Faster-RCNN, YOLOv7,
140 YOLOv8, CenterNet, SSD, RetinaNet, EfficientDet, Deformable-DETR, and DINO (DETR with

141 improved denoising anchor boxes).
142
143 The hyperparameter settings for these experiments and the backbone networks used by the models
144 are presented in Table 1. We compared different backbones with varying parameter quantities and
145 selected the best-performing one on our test set for each model. For instance, in the case of Faster-
146 RCNN, we compared ResNet50 and VGG16 as backbones and selected ResNet50 as its backbone.
147 We then chose the top-performing model based on its performance on the test set, which served as
148 the foundation for our subsequent experiments.

149

Model	Backbone	Batch size	Epoch	Learning rate	Optimizer
Faster-RCNN	ResNet-50	32	200	0.001	AdamW
YOLOv7	YOLOv7	32	200	0.01	AdamW
YOLOv8	YOLOv8m	32	200	0.01	AdamW
CenterNet	ResNet-101	32	200	0.04	AdamW
SSD	MobileNetV2	32	200	0.015	AdamW
RetinaNet	ResNet-101	32	200	0.0001	AdamW
EfficientDet	EfficientNet-B3	32	200	0.04	AdamW
Deformable-DETR	ResNet-50	32	200	0.0002	AdamW
DINO	4scale-Swin	8	200	0.0001	AdamW

150 Table 1. Hyperparameter settings for the different deep learning models

151
152 For the above nine models, 800 simulated wheat images were used for training, and 200 other
153 simulated wheat images were used for validation. We then tested these models on all the test sets
154 (1330 real wheat images) to identify the best performing model. This experiment also aimed to

155 verify whether the model trained on simulated wheat images could recognize real wheat images.
156 We used this training and optimization setup to obtain a model that performed well on the wheat
157 yield prediction task, with a view to exploring the practical applications of simulated wheat in
158 predicting the number of real wheat heads.

159

160 **4. Model testing**

161 We used a total of six indicators to test the performance of our model: R² (1), RMSE (2), MAE (3),
162 precision (4), recall (5), and F1-score (6). They were calculated as follows.

$$R^2 = 1 - \frac{\sum_{i=1}^n (\hat{y}_i - y_i)^2}{\sum_{i=1}^n (y_i - \bar{y})^2} \quad (1)$$

$$RMSE = \sqrt{\frac{1}{n} \sum_{i=1}^n (\hat{y}_i - y_i)^2} \quad (2)$$

$$MAE = \frac{1}{n} \sum_{i=1}^n |\hat{y}_i - y_i| \quad (3)$$

$$Precision = \frac{TP}{TP + FP} (iou = 0.5) \quad (4)$$

167

$$Recall = \frac{TP}{TP + FN} (iou = 0.5) \quad (5)$$

169

$$F1-score = \frac{2TP}{2TP + FP + FN} (iou = 0.5) \quad (6)$$

171

172 R² (1) was employed to assess the linear correlation between the predicted and ground truth values
173 for wheat head counts. RMSE (2) and MAE (3) were used to quantify the error between the

174 predicted and ground truth values. The precision (4), recall (5) and F1-score (6) were computed for
175 an intersection over union (IOU) of 0.5, which served as a reference for the recognition ability of
176 the model. In the formulae above, y_i represents the ground truth value for the number of wheat
177 heads in image i, \hat{y}_i represents the predicted number of wheat heads in image i, \bar{y} represents the
178 average number of actual wheat heads in all images, and n is the number of images used for testing.
179 TP is the count of actual wheat heads detected by the model, while TN represents the count of
180 objects correctly identified as non-wheat, which in this experiment was always zero. FP is the count
181 of objects predicted as wheat by the model that were not actually wheat, and FN denotes the count
182 of undetected wheat heads by the model.

183

184 The closer the values of R^2 , precision, recall, and F1-score, to one, the better the performance of
185 the model. For RMSE and MAE, a value closer to zero indicates better performance.

186

187 **5. Data size analysis**

188 To verify the effect of the size of the simulated wheat training dataset on the performance of the
189 model, we created eight scaled simulation datasets of 100, 200, 300, 400, 500, 600, 700, and 800
190 images for use in training. Each of these datasets was randomly selected and constructed from 800
191 simulation wheat images. To further test the performance of the model in different scenarios, we
192 also applied four image processing methods (light enhancement, light reduction, Gaussian blur, and
193 down sampling) to the test set and constructed four new test sets. In the case of Gaussian blur, we
194 set the blur kernel size to nine, whereas for down sampling, we resized the images using bilinear
195 interpolation to give a maximum side length of 512 pixels.

196

197 **6. Comparison of our simulation strategy with real wheat images**

198 To assess the effectiveness of our simulation strategy, we conducted training using two real wheat
199 datasets: the GWHD2021 training dataset, and 2500 images of green wheat from the SDAU2021

200 dataset. Specifically, for the GWHD2021 training dataset, we trained two models using the original
201 RGB channel and the channel after grayscale image processing, respectively. We then compared
202 the results based on the test set with those from the model trained on our simulated wheat dataset.

203

204 **7. Effects of the growth stage on model building**

205 To test the performance of the model in different growth periods, we extracted wheat images
206 collected on May 18th, May 23rd, June 1st and June 3rd from SDAU2023 test set, which illustrated
207 the process of wheat heads changing from green to yellow. We obtained 11, 10, 32, and 19 wheat
208 images for each date, and these 72 wheat images were used for testing with the best model.

209

210 **8. Overlapping of wheat heads**

211 To evaluate our model's performance in detecting overlapping wheat heads, we extracted 300
212 regions with obvious overlaps from the SDAU2021 to SDAU2024 test sets. These regions include
213 instances of 2, 3, and 4 wheat heads overlap. This set of images comprises 150 images from the
214 green stage of growth and 150 from the yellow stage. We used the trained YOLOv7 model to test
215 and assess its performance on both the green and yellow wheat images.

216

217 **Results**

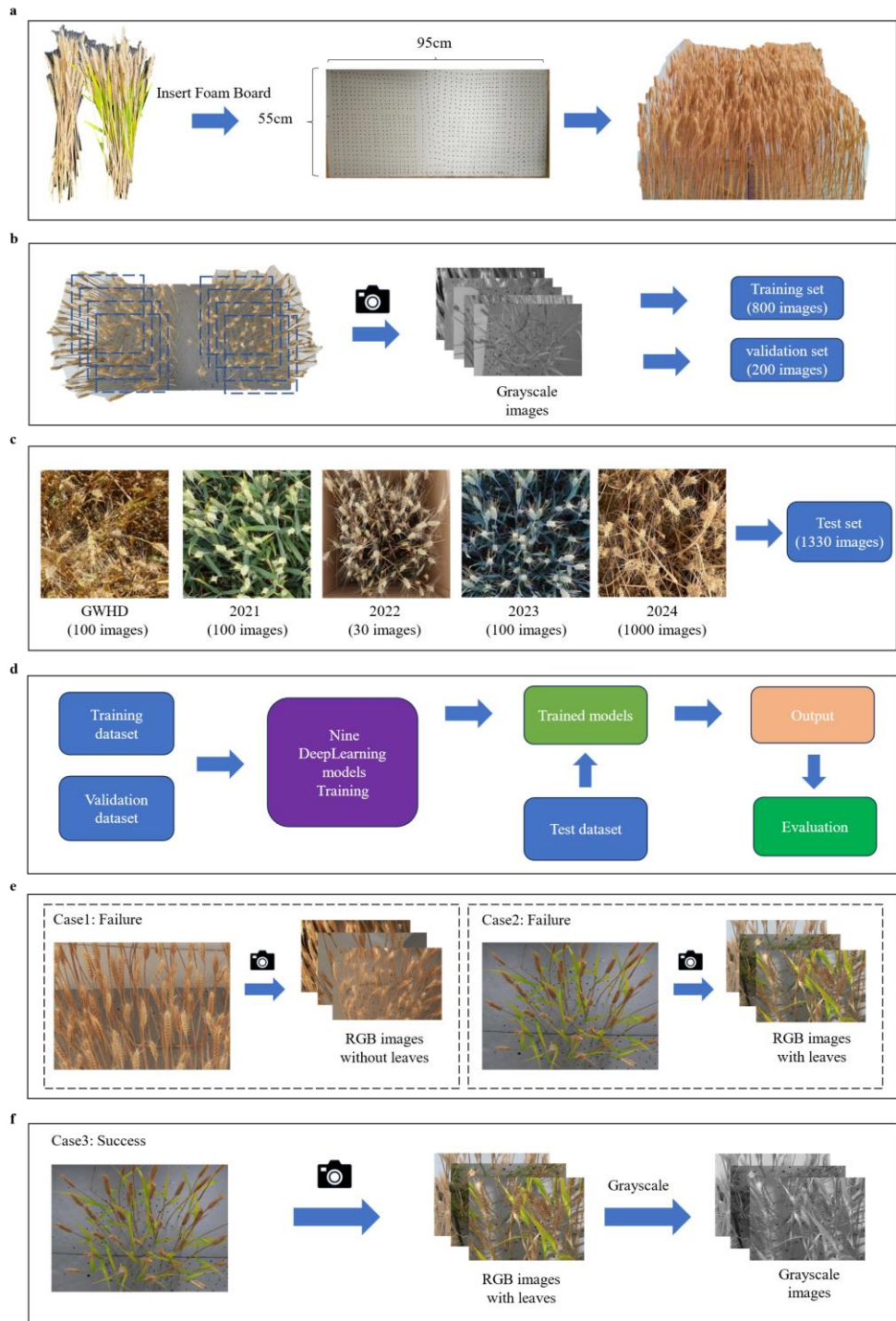
218 **1. Simulation workflow**

219 In this research, we used three components—air-dried wheat, simulated wheat leaves, and gray
220 foam board—to construct a simulation system for wheat at the stage of full maturity
221 (Supplementary Data 1). Firstly, since the selected air-dried wheat did not contain any leaves,
222 simulated wheat leaves were used to construct wheat-like plants. We used two gray foam boards as
223 the background, each of which had a length of 95 cm and a width of 55 cm. Using a punching tool,
224 we created holes in the foam board at intervals of 1 to 2 cm, for the insertion of wheat-like plants,
225 and then simulated wheat for training models (Fig. 1a). Next, image data were collected for wheat

226 in the simulated system. To ensure the high resolution of the image data, a Canon EOS 70D camera
227 was used for shooting, and a total of 1000 simulated images were taken. The images obtained in
228 this way were first cropped to remove the parts that were irrelevant to this experiment, such as the
229 floor and background, and grayscale image processing was then performed to reduce the influence
230 of the different colors of the wheat heads, the environment, and the camera setup on data processing
231 (Fig. 1b). In the next step, 200 simulated images were randomly chosen as a validation set, 100
232 images from GWHD2021 and 1230 images from SDAU2021-2024 were chosen as a test set (Fig.
233 1c). Finally, nine advanced deep learning models developed for the task of object detection were
234 selected for training and testing, including Faster-RCNN, YOLOv7, YOLOv8, CenterNet, SSD,
235 RetinaNet, EfficientDet, Deformable-DETR, and DINO (Fig. 1d).

236

237 For the preliminary experiment, we employed a subset of 100 images from the GWHD dataset as
238 the test set. Wheats in these images were in different colors, relatively high resolution and could be
239 recognized by human eye. We designed three distinct cases as follows: (1) Case 1: wheat only (Fig.
240 1e). In this case, we only used air-dried wheat. However, the performance of the model fell
241 considerably short of expectations, achieving an R^2 of only 0.744 and an RMSE of 11.822, results
242 that were far from satisfactory. (2) Case 2: wheat + leaves + weeds (Fig. 1e). To make the
243 background more complex, we introduced both leaves and weeds. The performance of the model
244 remained unsatisfactory, yielding an R^2 of 0.776 and an RMSE of 9.357. (3) Case 3: wheat + leaves
245 + weeds + grayscale image processing (Fig. 1f). In this final case, we converted RGB images to
246 gray images before training and testing the detection model to eliminate the lack of generalization
247 caused by simulating a single color and variety of wheat. The grayscale conversion was performed
248 using OpenCV's 'cvtColor' function, which employs the formula: gray channel = $0.299 \times \text{red} +$
249 $0.587 \times \text{green} + 0.114 \times \text{blue}$. It was interesting to note that this processing step led to a significant
250 enhancement in model performance, resulting in an impressive R^2 of 0.904 and a reduced RMSE
251 of 4.113.



252

253 **Fig. 1: Overview of simulation workflow**

254 **a** Simulated wheat field using gray foam boards and air-dried wheat. **b** Collection of simulated
255 wheat. **c** Composition of the test set. **d** Model comparison process. **e** Two cases of failed
256 experiments. **f** Successful experiment.

257

258 **2. Model comparison**

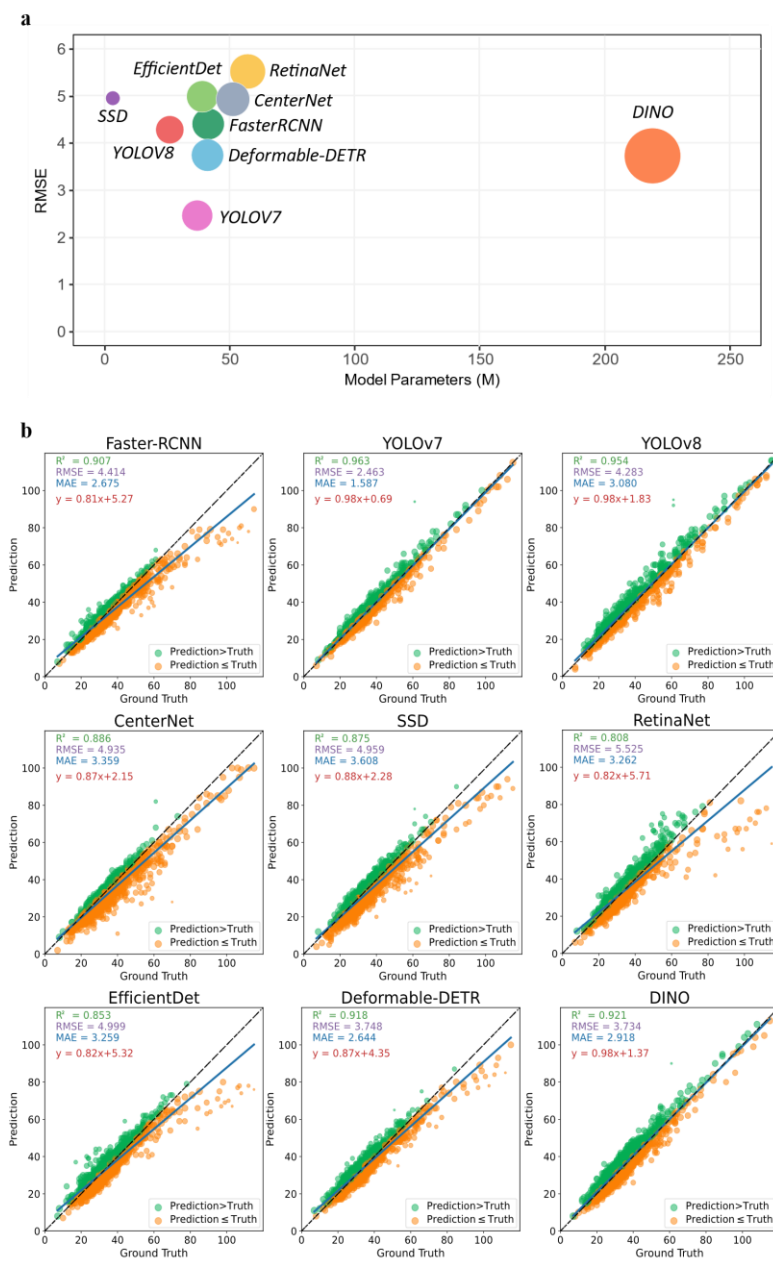
259 To train the model to count wheat heads, we partitioned the data as follows: 800 images sourced
 260 from the simulation were used for training, 200 images sourced from the simulation for validation,
 261 and 1330 images from the real wheat datasets for testing (Table 2). Our analysis considered nine
 262 diverse models: Faster-RCNN, YOLOv7, YOLOv8, CenterNet, SSD, RetinaNet, EfficientDet,
 263 Deformable-DETR, and DINO (Fig. 2c). The selection of these models was made for various
 264 reasons: Faster R-CNN and SSD previously exhibited satisfactory results in our prior research
 265 ([Geng et al., 2023](#)), while YOLOv7 and YOLOv8 were chosen due to their popularity and
 266 effectiveness in the object detection field. In view of the current prominence of Transformer-based
 267 models in object detection ([Beal et al., 2012](#)), we included two improved versions based on DETR
 268 ([Carion et al., 2020](#)), namely Deformable-DETR and DINO. In addition, CenterNet, RetinaNet,
 269 and EfficientDet were included due to their widespread use and success in the task of object
 270 detection.

Type	Source	Image Number	R ²	RMSE	MAE
Training	Simulation	800	-	-	-
Validation	Simulation	200	-	-	-
	GWHD	100	0.904	4.113	2.74
	SDAU2021	100	0.905	3.161	2.37
Test	SDAU2022	30	0.937	3.133	3.133
	SDAU2023	100	0.935	5.594	3.68
	SDAU2024	1000	0.949	1.709	1.258

271 Table 2. Training, validation and test sets.

272

273 The results indicated that YOLOv7 gave the highest performance on the test set, with an R^2 value
 274 of 0.963 and an RMSE of 2.463 (Fig. 2b) for the total 1330 real wheat images. Furthermore, it had
 275 a smaller number of parameters than the other models while maintaining high performance (Fig.
 276 2a). The success of YOLOv7 in terms of achieving superior performance on the test set not only
 277 underlines its accuracy but also its computational efficiency for the task of wheat head counting,
 278 which is essential for practical applications, especially in resource-constrained environments.



280 **Fig. 2. Model Comparison**

281 **a** Parameters number of nine models, and their root mean square error (RMSE) on the test dataset.

282 X-axis represents the number of model parameters (Million), Y-axis represents the RMSE values.

283 **b** Scatter plot of nine models between true number (X-axis) of wheat heads and predicted number

284 (Y-axis) of wheat heads on the test set.

285

286 The comparison results demonstrate the effectiveness of the simulation strategy. The use of these
287 diverse models and a comparative evaluation provides valuable insights into the evolving landscape
288 of object detection methodologies for agricultural purposes. Our choice of models ranged from
289 traditional ones such as Faster R-CNN to the more recent Transformer-based variants. This
290 adaptability is crucial to handle the varying complexities of real-world scenarios and opens avenues
291 for further exploration and optimization of agricultural computer vision applications.

292

293 **3. Data size selection**

294 To understand the effect of the size of the training dataset on the performance of the YOLOv7
295 model, we trained and tested the model with varying numbers of simulated wheat images: 100, 200,
296 300, 400, 500, 600, 700, and 800. We evaluated the model using five independent test sets (GWHD,
297 SDAU2021, SDAU2022, SDAU2023, SDAU2024) and observed that the model achieved
298 impressive R^2 and RMSE values when more than 500 images were used (Fig. 3a).

299

300 To further explore the robustness of the model, we systematically tested images under four different
301 preprocessing conditions (Fig. 3b): (i) light enhancement; (ii) light reduction; (iii) Gaussian blur;
302 and (iv) down sampling. These preprocessing conditions correspond to potential issues that may
303 arise when capturing images, including different lighting conditions, blurred and low-resolution
304 images. Notably, we found that light enhancement and light reduction did not significantly affect
305 the model's performance, with results comparable to those obtained with unprocessed images. For

example, with 800 images, the model achieved R^2 values of 0.931 for light enhancement and 0.955 for light reduction, similar to the control case. In contrast, the model exhibited a marked sensitivity to blur and low-resolution effects, indicating that low-quality images significantly impact model performance. Specifically, with Gaussian blur, the model achieved an R^2 value of only 0.88. Down sampling (low-resolution) had a similar effect, with the highest R^2 value reaching only 0.89.

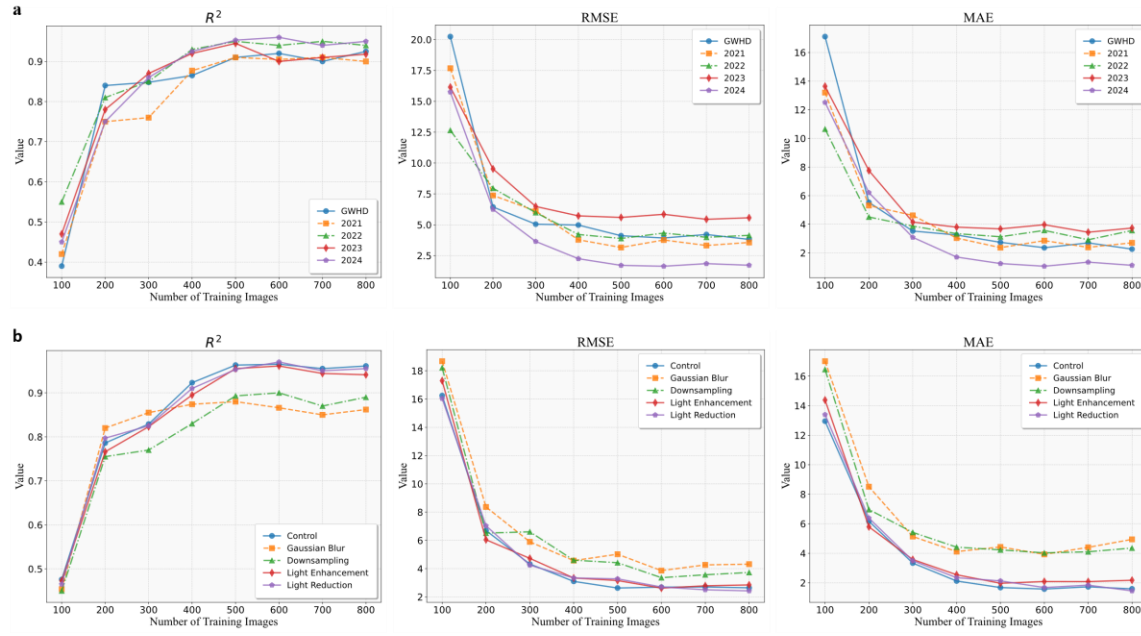


Fig. 3. Comparison of model performance trained with different numbers of simulated wheat images

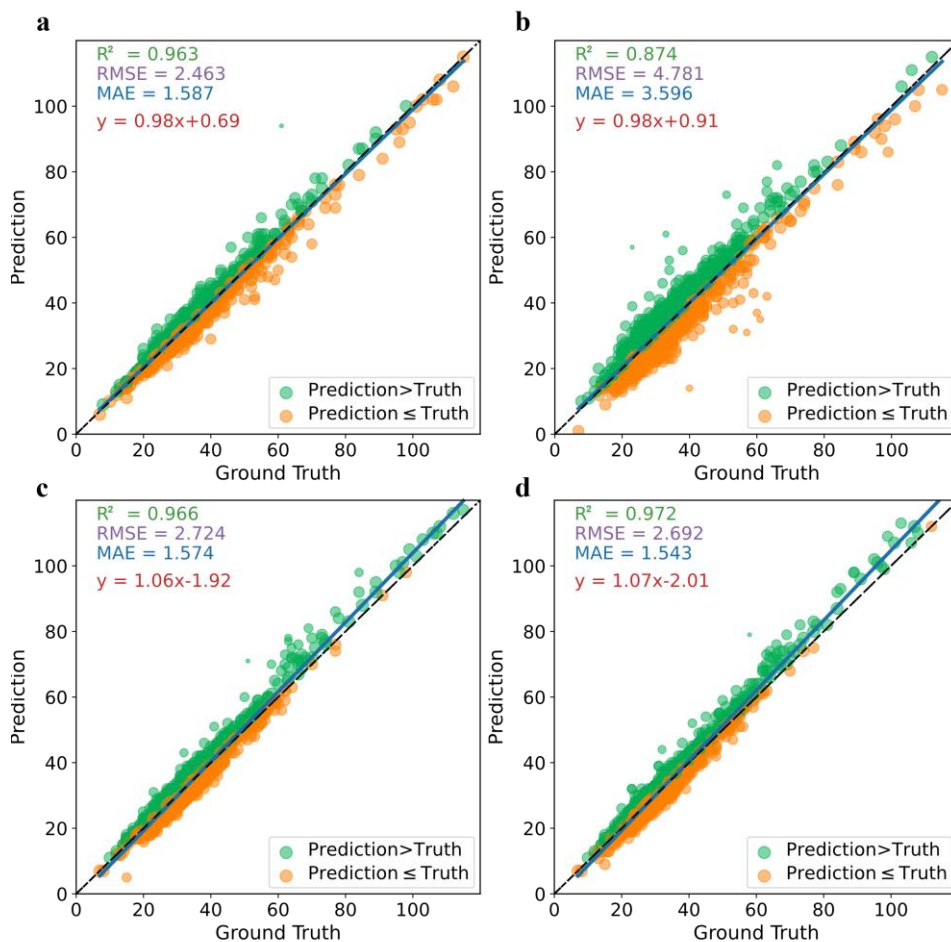
a Comparison of performance of YOLOv7 models trained with different numbers of images on five separate test sets (GWHD, SDAU2021-2024). **b** Comparison of performance of YOLOv7 models trained with different numbers of images on different processing conditions of the entire test set.

317

318 4. Comparison of our simulation strategy with real wheat images

319 To compare the effects of simulated and real images of wheat on the performance of the model, we
320 used two sets of real wheat data to train the YOLOv7 model: one contained 2500 images of green
321 wheat from SDAU2021, and the other was the GWHD2021 training dataset. For the former dataset,
322 we trained a model using the original RGB channel, while for the latter, we trained two models

323 using the original RGB channel and the channel after grayscale image processing, respectively. A
 324 comparative analysis of these models revealed that using our simulation strategy to train the model
 325 on 800 simulated wheat images (Fig. 4a) gave superior performance compared to the training the
 326 model on 2500 green wheat images from SDAU2021 (Fig. 4b); this model yielded similar RMSE
 327 and MAE values with the model trained on the GWHD2021 training set, which contained 3360
 328 wheat images. Furthermore, a comparison of the two models trained on the GWHD2021 dataset
 329 showed that the model trained on the channel without grayscale image processing (Fig. 4c)
 330 performed similarly to the model trained with grayscale image processing (Fig. 4d).



331

332 **Fig. 4. Simulated wheat versus real wheat**

333 **a** Test result of the YOLOv7 model trained with 800 simulated wheat images. Both the training and
 334 test images are processed by Grayscale image processing. **b** Test result of the YOLOv7 model

335 trained with 2500 green wheat images from SDAU2021. Both the training and test images are using
336 original RGB channel. **c** Test result of the YOLOv7 model trained with 3360 images in GWHD
337 training dataset. Both the training and test images are using original RGB channel. **d** Test result of
338 the model trained with 3360 images in GWHD training dataset. Both the training and test images
339 are processed by Grayscale image processing.

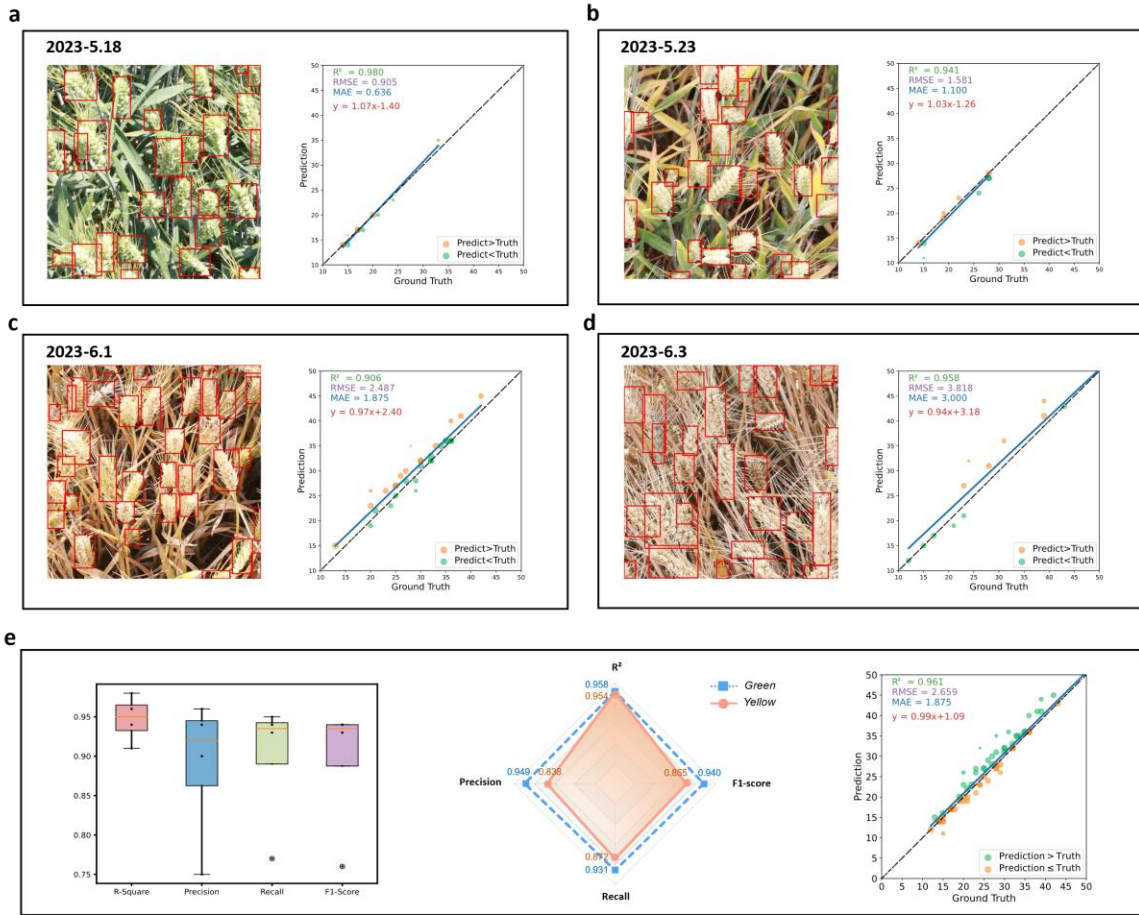
340

341 **5. Effects of the growth stage on model building**

342 To evaluate the performance of the model at different stages of growth of the wheat heads, we
343 systematically selected four dates over the growing season to capture both green wheat heads and
344 yellow ones, which were 17(Fig. 5a), 12(Fig. 5b), 3(Fig. 5c), and 1(Fig. 5d) days before harvest
345 (May 18th, May 23rd, June 1st and June 3rd, 2023). We found that all the R² values were higher than
346 0.9 and that none of the RMSE values exceeded 4. The highest accuracy was achieved for green
347 wheat heads, 17 days before harvest (June 3rd, 2023), with an R² of 0.980 and an RMSE of 0.905
348 (Fig. 5a). All of the metrics for the green wheat heads were better than for the yellow wheat heads,
349 demonstrating that color had a strong effect on model performance. We found that the RMSE and
350 MAE were worst on the last day before harvest, with an RMSE value of 3.818 and an MAE value
351 of 3, but the R² value was still higher than 0.9. Overall, we found that the R², RMSE and MAE
352 were satisfactory for the wheat images on these four different dates.

353

354 To determine the effect of color on the performance of the model, we split the wheat heads into two
355 groups: green (21 images) and yellow (51 images). Unexpectedly, all of the metrics for the green
356 images were better than those for the yellow images, thereby confirming the significant impact of
357 wheat growth period on model performance. Specifically, for green images, the values were 0.958
358 for R², 1.272 for RMSE, 0.857 for MAE, 0.949 for precision, 0.931 for recall, and 0.940 for F1-
359 score. The metrics for the yellow images were as follows: 0.954 for R², 3.052 for RMSE, 2.294 for
360 MAE, 0.838 for precision, 0.872 for recall, and 0.855 for F1-score (Fig. 5e).



361

362 **Fig. 5. Test results of different growth stages**

363 **a b c d** Test results on the images collected on four dates (May 18th, May 23rd, June 1st, June 3rd) **e**
 364 Box plot of test results on the four dates (left); Evaluation metrics of the green wheat images and
 365 yellow wheat images (center); Scatter plot of result for images from all the four dates (right).

366

367 **6. Overlapping of wheat heads**

368 To assess the performance of our models in scenarios involving overlapping wheat heads, we select
 369 two approaches (Supplementary Data 2): 1) Firstly, we chose 300 images with overlapping regions
 370 randomly from SDAU2021-SDAU2024. To understand the complexity of the overlapping, we
 371 manually divided the overlapping areas in these images as: A (2 wheat heads overlapping), B (3
 372 wheat heads overlapping), and C (4 wheat heads overlapping). Interestingly, we found these images

373 have a little bit lower R-square than that of the test data (Table 3). 2) Secondly, we selected 150
374 regions with overlapping wheat heads from 150 green wheat images, and 150 similar regions from
375 150 yellow wheat images. We also manually curated these regions into three classes: A (2 wheat
376 heads overlapping), B (3 wheat heads overlapping), and C (4 wheat heads overlapping). Overall,
377 the difference between the predicted values and the ground truth value was zero for 194 (64.6%)
378 of the regions, one for 100 regions, and two for 6 regions (Fig.6). Most of the predicted values for
379 the number of wheat heads in the images were the same as the ground truth, or only one lower than
380 the ground truth.

381

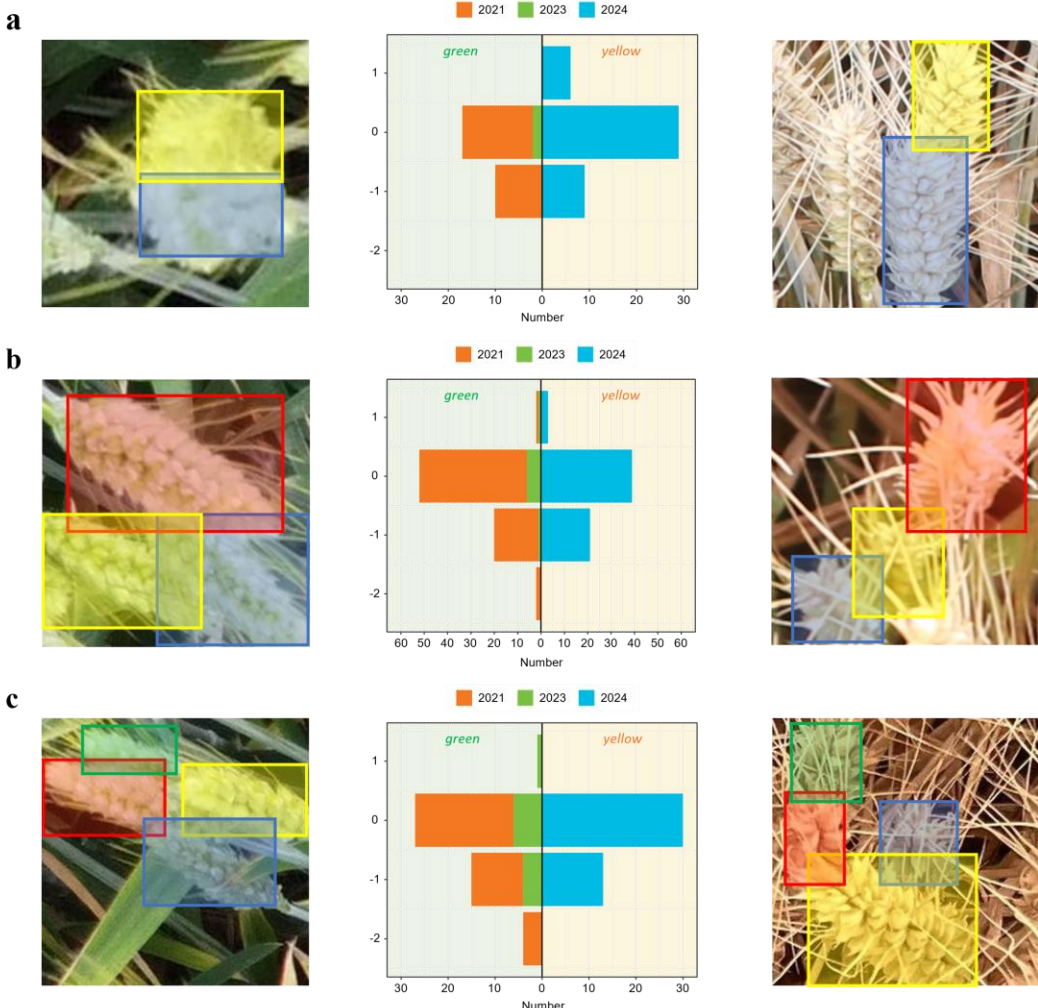
382 The minor differences between the predicted number of wheat heads and the ground truth values
383 demonstrate the effectiveness of the model in dealing with overlapping wheat heads. The
384 effectiveness in processing overlapping regions can be attributed to our simulation strategy, which
385 included simulations of overlapping cases, enhancing the model's ability to predict on similar cases
386 in the test sets.

387

Datasets	Overlapping region of at least one wheat head < 50%			Overlapping region of at least one wheat head > 50%			Image Number	True number	Predicted number	R ²
	A	B	C	A	B	C				
SDAU2021	31	16	9	6	0	1	29	1757	1733	0.865
SDAU2022	29	15	3	13	5	0	37	2526	2478	0.938
SDAU2023	49	22	3	34	25	2	49	2312	2445	0.908
SDAU2024	172	100	51	123	92	36	185	5745	5781	0.894

388 Table 3. Test results on images with overlapping regions

390



391

392 **Fig. 6. Analysis of wheat overlapping regions**

393 **a** Regions with two wheat heads overlapping. **b** Regions with three wheat heads overlapping. **c**

394 Regions with four wheat heads overlapping.

395

396 **Discussion**

397 In this work, we designed a simulation strategy to count wheat heads. When 800 simulated images
 398 were used, we achieved values of 0.963 for R^2 and 2.463 for RMSE with YOLOv7. To further test
 399 our model, we chose five different datasets, GWHD2021, SDAU2021, SDAU2022, SDAU2023,
 400 SDAU2024, each of which gave similar results. We also utilized two data sets randomly selected
 401 from Kaggle (<https://www.kaggle.com/>) (Supplementary Data 3). These tests demonstrated that the

402 proposed simulation model worked very well in terms of counting wheat heads. We also found that
403 our model was not affected by the different growth stages or colors of wheat. Finally, our results
404 showed that the model worked well in cases with overlapping wheat heads.

405

406 The simulation strategy was proven successful in microscope images ([Shin et al., 2024](#)). In this
407 work, we extended this approach to precision agriculture, which proved to be effective. The
408 advantages of the proposed simulation strategy are as follows. First, when a simulation pipeline is
409 used, there is no need to limit the collection time to a very short, agriculturally determined period,
410 and the simulation period can theoretically be extended as long as desired. The whole pipeline can
411 be applied anywhere and at any time, which can greatly decrease the research time needed from
412 one or two years to one or two months. In addition, it enables tests under different agricultural
413 conditions with different experimental designs, which may be very hard to collect or rare (i.e., an
414 occurrence every two or more years). Finally, the limitations of field work mean that some data are
415 not possible to collect and there is a strong reliance on image data, which may not be true values.
416 For example, the true number of wheat heads in images is hard to determine, and the use of
417 inaccurate data is harmful to the performance of the model ([Chen et al., 2023](#)). The availability of
418 high-quality labeled datasets is crucial for the performance of deep learning models ([Shermeyer et](#)
419 [al., 2019](#)). With a simulation pipeline, we can guarantee that the ground truth data are accurate at
420 the model training stage, thus improving the performance of the model.

421

422 In addition, this strategy means that a large number of wheat datasets can be collected within a very
423 short time. By constructing a simulated wheat growth system, a large-scale dataset can be quickly
424 established, which not only effectively avoids the tedious processes of on-site sampling and data
425 collection but also shortens the time needed for data acquisition. In general, thousands of images
426 are needed to achieve satisfactory accuracy with real data; in contrast, in this work, we used 800
427 high-quality images collected from simulations, and the threshold was 200 images for evaluation

428 metrics: R^2 , RMSE and MAE. As a result, this approach can save labor and effort.

429

430 In our previous study, the different stages of growth and colors of the wheat heads had a strong
431 effect on the selection (Geng et al., 2023) and performance of the model. In this work, we
432 systematically collected image data at different growth stages of the wheat, with different colors.
433 After applying grayscale image processing, we achieved similar values for the accuracy and
434 precision for the different growth stages with varying colors. This finding supports the idea that the
435 use of data processing, such as grayscale processing, can overcome this challenge.

436

437 The simulation strategy proposed in this work was shown to be effective and can also be applied to
438 other aspects of precision agriculture. In future work, we will use the simulation model to test
439 various other areas of precision agriculture, including crop logging, fruit or leaf counting, and weed
440 identification and classification. We believe that this powerful approach could be extended to all
441 fields of precision agriculture, and can achieve highly accurate results within a very short time.

442

443 **Data availability**

444 All of our experimental data including simulated and real datasets can be downloaded from
445 https://figshare.com/articles/dataset/Untitled_Item/24198891.

446

447 **Code availability**

448 All of our experimental codes can be found at <https://github.com/gyhdc/wheat-simulation>.

449

450 **References**

451 Balfourier, F., Bouchet, S., Robert, S., De Oliveira, R., Rimbert, H., Kitt, J., Choulet, F., Paux, E.,
452 2019. Worldwide phylogeography and history of wheat genetic diversity. Sci. Adv. 5, eaav0536.
453 Beal, J., Kim, E., Tzeng, E., Park. D. H., Zhai, A., Kislyuk, D., 2020. Toward transformer-based

- 454 object detection. arXiv preprint arXiv:2012.09958.
- 455 Carion, N., Massa, F., Synnaeve, G., Usunier, N., Kirillov, A., Zagoruyko, S., 2020. End-to-end
456 object detection with transformers. ECCV. pp. 213-229.
- 457 Chen, X., Li, M., Zhang, J., Xia, X., Wei, C., Cui, J., Gao, X., Zhang, X., Yan, R., 2023. Learning
458 towards Selective Data Augmentation for Dialogue Generation. arXiv preprint arXiv:2303.09719.
- 459 Dandrifosse, S., Ennadifi, E., Carlier, A., et al., 2022. Deep learning for wheat ear segmentation
460 and ear density measurement: From heading to maturity. Computers and Electronics in Agriculture.
461 199, 107161.
- 462 Darwin, B., Dharmaraj, P., Prince, S., et al., 2021. Recognition of bloom/yield in crop images using
463 deep learning models for smart agriculture: A review. Agronomy.11, 646.
- 464 David, E., Madec, S., Sadeghi-Tehran, P., Aasen, H., Zheng, B., Liu, S., Klrgessner, N., Ishikawa,
465 G., Nagasawa, K., Badhon, M., et al. 2020. Global Wheat Head Detection (GWHD) dataset: a large
466 and diverse dataset of high-resolution RGB-labelled images to develop and benchmark wheat head
467 detection methods. Plant Phenomics, 3521852.
- 468 David, E., Ogidi, F., Smith, D., Chapman, S., de Solan, B., Guo, W., Baret, F., Stavness, I., 2023.
469 Global wheat head detection challenges: winning models and application for head counting. Plant
470 Phenomics. 5, 0059.
- 471 Dhankher, O. P., Foyer, C. H., 2018. Climate resilient crops for improving global food security and
472 safety. Plant Cell Environ. 41, 877-884.
- 473 Duan, K., Bai, S., Xie, L., Qi, H., Huang, Q., Tian, Q., 2019. Centernet: Keypoint triplets for object
474 detection. ICCV Proc. IEEE Int. Conf. Comput. Vis. pp. 6569-6578.
- 475 Fernandez-Gallego, J.A., Buchaillot, M.L., Aparicio Gutiérrez, N., et al., 2019. Automatic wheat
476 ear counting using thermal imagery. Remote Sens. 11, 751.
- 477 Fernandez-Gallego, J.A., Kefauver, S.C., Gutiérrez, N.A., et al., 2018. Wheat ear counting in-field
478 conditions: high throughput and low-cost approach using RGB images. Plant Methods. 14, 22.
- 479 Fernandez-Gallego, J.A., Lootens, P., Borra-Serrano, I., et al., 2020. Automatic wheat ear counting

480 using machine learning based on RGB UAV imagery. *Plant J.* 103, 1603-1613.

481 Geng, X., Zuo, C., Zhao, Q., Hao, J., Wang, Y., Tang, Z., Sun,X., 2023.

482 Analyzing Spatial Distribution Patterns of Wheat Ears. ICIVC. pp. 76-86.

483 Gupta, A., Hua, L., Zhang, Z., Yang, B., Li, W., 2023. CRISPR-induced miRNA156-recognition

484 element mutations in TaSPL13 improve multiple agronomic traits in wheat. *Plant Biotechnol J.* 21,

485 536-548 .

486 Hartley, Z.K.J., French, A.P., 2021. Domain adaptation of synthetic images for wheat head

487 detection. *Plants.* 10, 2633.

488 Huang, H., Huang, J., Feng, Q., Liu, J., Li, X., Wang, X., et al., 2022. Developing a dual-stream

489 deep-learning neural network model for improving county-level winter wheat yield estimates in

490 China. *Remote Sens.* 14, 5280.

491 Lev-Mirom, Y., Distelfeld, A., 2023. Where was wheat domesticated. *Nat. Plants* 9, 1201-1202.

492 Li, L., Hassan, M.A., Yang, S., Jing, F., Yang, M., et al., 2022. Development of image-based wheat

493 spike counter through a Faster R-CNN algorithm and application for genetic studies. *The Crop*

494 *Journal.* 10, 1303-1311.

495 Lin, T.Y., Goyal, P., Girshick, R., He, K., Dollár, P., 2017. Focal loss for dense object detection.

496 Proc. IEEE Int. Conf. Comput. Vis. 42, 2980-2988.

497 Liu, C., Wang, K., Lu,H., Cao.Z., 2022, Dynamic Color Transform Networks for Wheat Head

498 Detection. *Plant Phenomics.*2022, 9818452.

499 Liu, S., Peng, D., Zhang, B., Chen, Z., Yu, L., Chen, J., Pan, Y., Zheng, S., Hu, J., Lou, Z., 2022.

500 The accuracy of winter wheat identification at different growth stages using remote sensing.

501 *Remote Sens.* 14, 893.

502 Liu, T., Wu, W., Chen, W., Sun, C., Zhu, X., Guo,W., 2016. Automated image-processing for

503 counting seedlings in a wheat field. *Precision Agric.* 17, 392-406.

504 Liu, W., Anguelov, D., Erhan, D., Szegedy, C., Reed, S., Fu, C., Berg, A., 2016. Ssd: Single shot

505 multibox detector. *ECCV.* pp. 21-37.

- 506 Long, D. S., McCallum, J. D., 2015. On-combine, multi-sensor data collection for post-harvest
507 assessment of environmental stress in wheat. *Precis Agric.* 16, 492-504.
- 508 Madec, S., Jin, X., Lu, H., Solan, B. D., Liu, S., Duyme, F., Herititer, E., Baret, F., 2019. Ear density
509 estimation from high resolution RGB imagery using deep learning technique. *Agric. For. Meteorol.*
510 264, 225-234.
- 511 Myers, S.S., Smith, M.R., Guth, S., Golden, C.D., Vaitla, B., Mueller, N.D., Dangour, A.D.,
512 Huybers, P., 2017. Climate change and global food systems: potential impacts on food security and
513 undernutrition. *Annu. Rev. Public Health.* 38, 259-277.
- 514 Ren, S., He, K., Girshick, R., Sun, J., 2017. Faster r-cnn: Towards real-time object detection with
515 region proposal networks. *IEEE Trans Pattern Anal Mach Intell.* 28, 1137-1149.
- 516 Rezaei, E.E., Webber, H., Asseng, S. et al. 2023. Climate change impacts on crop yields. *Nat. Rev.*
517 *Earth Environ.* 4, 831-846.
- 518 Romanovska P, Schauberger B, Gornott C. 2023. Wheat yields in Kazakhstan can successfully be
519 forecasted using a statistical crop model. *European Journal of Agronomy.* 147, 126843.
- 520 Sadeghi-Tehran, P., Virlet, N., Ampe, E. M.,Reyns, P., 2019. DeepCount: in-field automatic
521 quantification of wheat spikes using simple linear iterative clustering and deep convolutional neural
522 networks. *Front Plant Sci.* 10, 1176 .
- 523 Shermeyer, J., Van, Etten. A., 2019. The effects of super-resolution on object detection performance
524 in satellite imagery. *Proc. IEEE Conf. Comput. Vis. Pattern Recognit. Workshops.* pp. 1432-1441.
- 525 Shin, Y., Lowerison, MR., Wang, Y., Chen, X., You, Q., Dong, Z., Anastasio, M.A.,Song, P., 2024.
526 Context-aware deep learning enables high-efficacy localization of high concentration microbubbles
527 for super-resolution ultrasound localization microscopy. *Nat Commun.* 15, 2932.
- 528 Sun, C., Hu, H., Cheng, Y., Yang, X., Qiao, Q., et al., 2023. Genomics-assisted breeding: The next-
529 generation wheat breeding era. *Plant Breeding,* 142, 259-268.
- 530 Tan, M., Pang, R., Le, Q. V., 2020. Efficientdet: Scalable and efficient object detection. *Proc. IEEE*
531 *Conf. Comput. Vis. Pattern Recognit.* pp. 10781-10790.

- 532 Tesfaye, K., 2021 Climate change in the hottest wheat regions. Nat. Food 2, 8-9.
- 533 The labelImg program. <https://github.com/HumanSignal/labelImg>.
- 534 Wang, C. Y., Bochkovskiy, A., Liao, H. Y. M., 2023. YOLOv7: Trainable bag-of-freebies sets new
535 state-of-the-art for real-time object detectors. Proc. IEEE Conf. Comput. Vis. Pattern Recognit. pp.
536 7464-7475.
- 537 Wang, D., Zhang, D., Yang, G., Xu, B., Luo, Y., Yang, X., 2021. SSRNet: In-field counting wheat
538 ears using multi-stage convolutional neural network. IEEE Trans. Geosci. Remote Sens. 60, 1-11.
- 539 Wu, W., Zhong, X., Lei, C., Zhao, Y., Liu, T., Sun, C., Guo, W., Sun, T., Liu, S, 2023. Sampling
540 Survey Method of Wheat Ear Number Based on UAV Images and Density Map Regression
541 Algorithm. Remote Sens. 15, 1280.
- 542 Xu, X., Li, H., Yin, F., Xi, L., Qiao, H., Ma, Z., Shen, S., Jiang, B., Ma, X., 2020. Wheat ear counting
543 using K-means clustering segmentation and convolutional neural network. Plant Methods. 16, 1-13.
- 544 Yue, J., Feng, H., Jin, X., Yuan, H., Li, Z., Zhou, C., Yang, G., Tian, Q., 2018. A comparison of crop
545 parameters estimation using images from UAV-mounted snapshot hyperspectral sensor and high-
546 definition digital camera. Remote Sens. 10, 1138.
- 547 Zhang, H., Li, F., Liu, S., Zhang, L., Su, H., Zhu, J., Ni, L.M., Shum, H.Y., 2022. Dino: Detr with
548 improved denoising anchor boxes for end-to-end object detection. arXiv preprint
549 arXiv:2203.03605.
- 550 Zhao, Y., Tao, L., Tianle, Y., Chengxin, J., Chengming, S., 2022. Rapid detection of wheat ears in
551 orthophotos from unmanned aerial vehicles in fields based on YOLOX. Front. Plant Sci., 13,
552 851245.
- 553 Zhou, C., Liang, D., Yang, X., et al., 2018. Wheat ears counting in field conditions based on multi-
554 feature optimization and TWSVM. Frontiers in plant science. 9, 1024.
- 555 Zhu, X., Su, W., Lu, L., Li, B., Wang, X., Dai, J., 2020. Deformable detr: Deformable transformers
556 for end-to-end object detection. arXiv preprint arXiv:2010.04159.
- 557 Zhu, Y., Cao, Z., Lu, H., Li, Y., Xiao, Y., 2016. In-field automatic observation of wheat heading

558 stage using computer vision. Biosystems Engineering, 143, 28-41.

559

560 **Acknowledgements**

561 This research was funded by the Shandong Provincial Natural Science Foundation under Grant
562 ZR2021MC168 and partly by the National Natural Science Foundation of China under Grant
563 32070684, 31571306. We thank Dr. Xiaoliang Dong (Supercomputing Center, SDAU), Prof. Anfei
564 Li (Agricultural Experimental Station, SDAU) for their advices. We thank Supercomputing Center
565 in Shandong Agricultural University for technical support.

566

567 **Author contributions**

568 L.K. supervised this study. L.K. and X.S. conceptualized and designed this study. X.S., Q.L., Z.T.,
569 Y.Z., J.H., C. Z., X.G. participated in the data collection. T.J., Y.G., Y.W., J.H. performed the
570 analyses. All authors wrote and edited the manuscript.

571

572 **Competing interests**

573 The authors declare no competing interests.

Declaration of interests

The authors declare that they have no known competing financial interests or personal relationships that could have appeared to influence the work reported in this paper.

Author contributions

L.K. supervised this study. L.K. and X.S. conceptualized and designed this study. X.S., Q.L., Z.T., Y.Z., J.H., C. Z., X.G. participated in the data collection. T.J., Y.G., Y.W., J.H. performed the analyses. All authors wrote and edited the manuscript.



Click here to access/download
Supplementary Material
Supplementary_Data1.docx



Click here to access/download
Supplementary Material
Supplementary_Data2.xlsx



Click here to access/download
Supporting File
fig1.svg



Click here to access/download
Supporting File
fig2.svg



Click here to access/download
Supporting File
fig3.svg



Click here to access/download
Supporting File
fig4.svg



Click here to access/download
Supporting File
fig5.svg



Click here to access/download
Supporting File
fig6.svg



Click here to download Research Data
<https://figshare.com/s/62c2aab5fd1866c7423e>

